

# Numerical simulation of grain-size effects on creep crack growth by means of grain elements

P.R. Onck and E. van der Giessen

*Koiter Institute, Delft University of Technology, Mekelweg 2, 2628 CD Delft, The Netherlands*

**Abstract:** The effect of grain size on creep crack growth is investigated by means of a numerical technique in which the actual crack growth process is simulated in a discrete manner by grain elements and grain boundary elements. The grain elements account for the creep deformation of individual grains, while grain boundary cavitation and sliding are accounted for by grain boundary elements between the grains. This grain-element technique allows for an independent study of multiple grain size effects: a (direct) size effect related to the specimen size/grain size ratio or an (indirect) effect related to the effect of grain size on nucleation rate and creep resistance. Preliminary numerical results are presented concerning the direct effect of grain size, which predict that the crack growth rate and brittleness increase with grain size.

## 1 INTRODUCTION

The role of grain size in the plastic behaviour of polycrystalline materials at ambient temperatures has been studied extensively, resulting in the famous Hall-Petch relation. However, at high temperatures the strengthening effect of grain boundaries is counteracted by the weakening effect of typical high-temperature mechanisms like grain boundary sliding, diffusion and cavitation.

Deformation experiments show (e.g. [1]) that for a certain stress and temperature, there exists an optimal grain size for which the secondary-creep rate is minimal (see Fig. 1). While the positive slope in the creep-rate vs. grain-size curve is usually related to a Hall-Petch effect, for the negative slope a number of explanations have been given, depending on the applied stress and temperature: (i) grain boundary sliding (e.g. [2]), (ii) diffusional creep (e.g. [3, 4]), (iii) recovery along prior austenite grain boundaries (e.g. [5]), (iv) the presence of sub-grain boundaries (e.g. [6]).

Creep rupture experiments show that increasing the grain size results in smaller fracture strains, while the lifetime of the material decreases. Similar observations are reported in creep crack growth experiments, where an increase in grain size results in more brittle fracture and a higher crack growth rate. Explanations can be divided into two classes. First, it has been argued that the cavity nucleation rate tends to increase with grain size. This is related either to the larger sliding displacement in coarse-grained materials (e.g. [7, 8]) or to a higher density of second-phase particles resulting from the heat treatment to produce the coarse grain size (e.g. [8, 9]). A second class of explanations relates the observations to the fact that triple grain junctions can act as barriers to crack growth (e.g. [6, 10, 11]).

Most of the cited creep fracture experiments have been done on equal-sized specimens where different grain sizes have been obtained by varying the heat treatment of the material. However, this may change the material properties (e.g. nucleation rate, creep resistance), which obscures the explicit size effect related to the specimen length/grain size ratio. An approach that does not suffer from this artefact is one where specimens of different sizes are cut from the same material. This has been done by Hayhurst and co-workers [12, 13] who found that the lifetime was decreased by increasing the specimen size. This observation is not consistent with the trends found in the above cited experiments, but can be partly explained from the fact that the energy release rate was larger for the larger specimen.

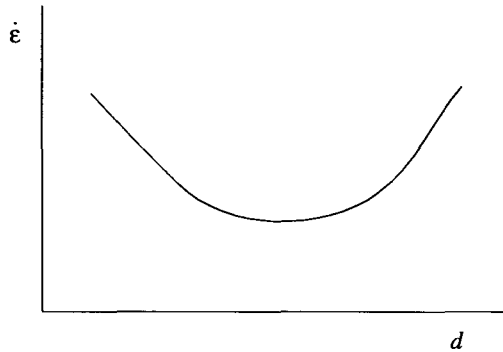


Figure 1: Schematic dependence of steady state creep rate  $\dot{\epsilon}$  on grain size  $d$  as observed in experiments.

The objective of the present study is to gain some understanding of the various observed phenomena in experiments on (grain) size effects, by simulations with a microstructural model for creep fracture. This model was recently developed by the authors as a new approach to describe creep crack growth. The idea is to represent the polycrystalline material by so-called grain elements. A grain element is a special-purpose finite element that describes the elastic and creep deformation of an individual grain, while cavitation and grain boundary sliding are accounted for by grain boundary elements between adjacent grains. In this way, intergranular creep crack growth can be simulated in a discrete manner, yet directly based on the polycrystalline microstructure and micro-scale physical mechanisms. The grain size is an insoluble and natural element of this model and offers the ability to study the direct effect of grain size.

In this paper, numerical results are presented in terms of crack growth rates as a function of grain size. In order to separate the various potential contributions to the grain-size effect on creep fracture, these first calculations account only for the effect of grain size through grain boundary sliding and the cavity growth process. The indirect effects of grain size on creep resistance and nucleation rate are discussed in terms of characteristic time scales governing creep crack growth.

## 2 MICROSTRUCTURAL MODEL

Here we only briefly summarize the model; full details can be found in [14, 15].

### 2.1 Constitutive equations

Obviously, the elastic and creep behaviour of individual grains is highly anisotropic. Averaged over a sufficiently large aggregate of random grains the behaviour becomes isotropic and creep is often described by the power law  $\dot{\epsilon}_e^C = B\sigma_e^n$ , where  $B$  is a material constant,  $n$  the creep exponent and  $\sigma_e$  the Mises stress. Representing the anisotropic creep behaviour of random individual grains would introduce a significant stochastic effect in the microstructural model which would complicate the interpretation of the fracture process enormously. Therefore, as in [16, 17, 18, 19], we assume that the material inside the grains is homogeneous and isotropic, and that creep is described by the power law based on average properties.

Grain boundary sliding is modelled by a Newtonian viscous relationship with viscosity  $\eta_B$ . In this paper, the grain boundary viscosity is expressed in terms of the strain rate parameter

$$\dot{\epsilon}_B = \left( \frac{w B^{-1/n}}{d \eta_B} \right)^{n/(n-1)}, \quad (1)$$

with  $w$  the thickness of the boundary and  $d$  a length parameter, related to the grain size. Effectively, grain boundary sliding can be characterized by the ratio  $\dot{\epsilon}_e^C/\dot{\epsilon}_B$ , denoting the relative resistance of the grain material and grain boundary layer. Free sliding ( $\eta_B = 0$ ) corresponds to  $\dot{\epsilon}_e^C/\dot{\epsilon}_B = 0$  and no sliding ( $\eta_B \rightarrow \infty$ ) to  $\dot{\epsilon}_e^C/\dot{\epsilon}_B \rightarrow \infty$ .

The cavitation process on the grain boundary facets is governed by the nucleation, growth and coales-

cence of cavities. The cavities are characterized by their radius  $a$  and half-spacing  $b$ . The average separation between two adjacent grains is specified by  $\delta_c = V/(\pi b^2)$  where  $V$  is the cavity volume. We adopt a smeared-out approach in which the discrete distribution of cavities is replaced by a continuous distribution. The rate of separation between the two adjacent grains,

$$\dot{\delta}_c = \frac{\dot{V}}{\pi b^2} - \frac{2V}{\pi b^2} \frac{\dot{b}}{b}, \quad (2)$$

is determined by the volumetric growth rate  $\dot{V}$  of the cavities and the rate of change of the cavity spacing  $\dot{b}$ . The growth rate  $\dot{V}$  is a result of grain boundary diffusion (controlled by the grain boundary diffusion parameter  $\mathcal{D}$ ) as well as of creep flow of the surrounding material and depends on the local stress state and damage level. This can be written in the functional form (e.g. [16, 17])

$$\dot{V} = \dot{V}_{\text{dif}}(\mathcal{D}, \sigma_n, a, b) + \dot{V}_{\text{cr}}(\sigma_m, \sigma_e, a), \quad (3)$$

where  $\dot{V}_{\text{dif}}$  and  $\dot{V}_{\text{cr}}$  are the contributions by diffusion and creep, respectively. Furthermore,  $\sigma_n$  is the average stress normal to the grain boundary, and  $\sigma_m$  and  $\sigma_e$  are the average mean and Mises stress, respectively, remote from the cavities. Needleman and Rice [16] introduced the length scale  $L = (\mathcal{D}\sigma_e/\dot{\epsilon}_e^C)^{1/3}$ , which governs the relative contribution of diffusion and creep to void growth. For small values of  $a/L$  (say,  $a/L < 0.1$ ) cavity growth is dominated by diffusion, while for larger values of  $a/L$  creep growth becomes more and more important.

The cavity spacing, represented by  $b$ , changes in the course of the failure process due to the nucleation of new cavities, and its rate of change is determined by

$$\dot{b}/b = -\frac{1}{2}\dot{N}/N, \quad (4)$$

in terms of the rate of change of the cavity density  $N$ . In this paper, we have used the nucleation law

$$\dot{N} = F \left( \frac{\sigma_n}{\Sigma_0} \right)^2 \dot{\epsilon}_e^C, \quad \text{for } \sigma_n > 0, \quad (5)$$

in conjunction with a threshold value  $S_{\text{thr}} = N_1/F$  for the accumulated quantity  $S = (\sigma_n/\Sigma_0)^2 \epsilon_e^C$ . Here,  $N_1$  is the initial cavity density and it is assumed that cavity nucleation is saturated when  $N = N_{\text{max}}$ .

## 2.2 Computational model

We adopt a boundary layer approach by prescribing the steady-state HRR-field,

$$\sigma_{ij} = \left[ \frac{C^*}{BI_n r} \right]^{1/(n+1)} \tilde{\sigma}_{ij}(\theta, n), \quad (6)$$

as the remote boundary condition as well as the initial condition, thus assuming that all elastic transients have relaxed before damage develops. Here,  $r$  and  $\theta$  are polar coordinates centered at the mathematical sharp crack tip,  $I_n$  is an  $n$ -dependent dimensionless constant,  $C^*$  the amplitude and  $\tilde{\sigma}_{ij}(\theta, n)$  a dimensionless function. The far-field region is treated by a standard finite element description of creep and elasticity, consisting of rings of 'crossed triangle' quadrilaterals (Fig. 2a). At the crack tip a rectangular process window is identified (Fig. 2b) within which the actual microstructure is represented by so-called grain elements and grain boundary elements [14]. The grain elements account for the elasticity and creep of the individual grains, while grain boundary sliding and cavitation is incorporated through grain boundary (interface) elements.

## 3 RESULTS

To investigate the influence of grain shape, we start out by considering a reference case with a half facet length  $R_0$  and corresponding grain diameter  $d_0 = 3.64R_0$  ( $d_0$  is the diameter of a circle whose area is the

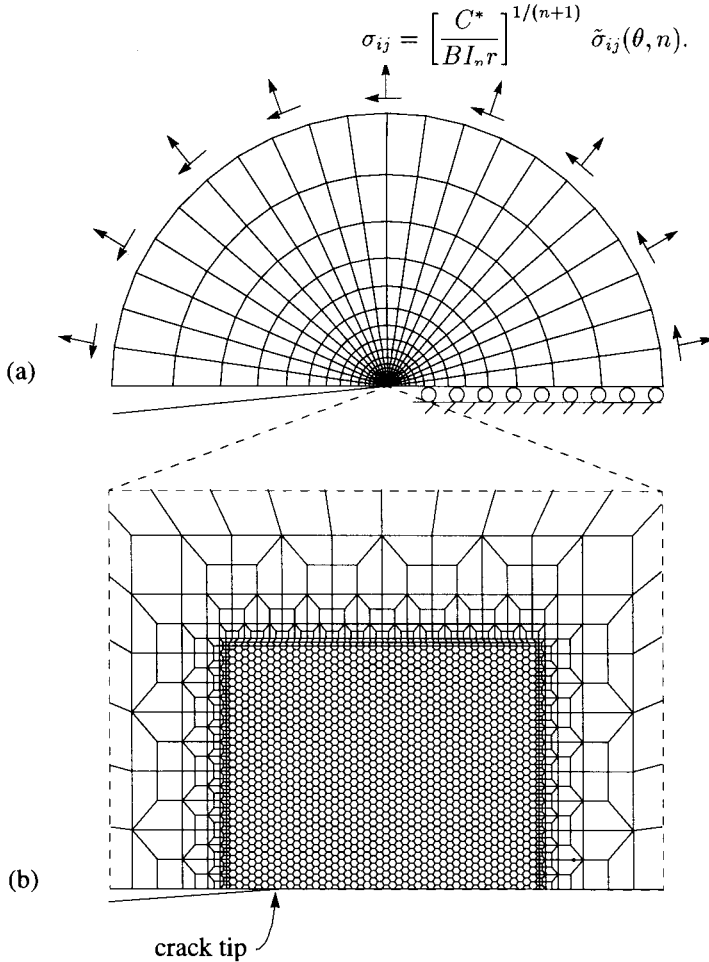


Figure 2: Finite element mesh used for small-scale damage analysis. (a) Circular domain with boundary conditions. (b) Crack tip region, showing the process window which consists of grain elements and grain boundary elements. Cavitation damage is allowed to occur along all grain boundaries in the process window.

same as a hexagonal grain with half facet length  $R_0$ ). We choose the following set of non-dimensional parameters:  $n = 5$ ,  $\Sigma_0/E = 0.9 \times 10^{-3}$ ,  $\dot{E}_0/\dot{\epsilon}_{B0} = 10$ ,  $N_I/N_0 = 40$ ,  $a_I/R_0 = 0.67 \times 10^{-3}$ ,  $a_I/L_0 = 0.02$ ,  $F_0/N_0 = 2.4 \times 10^3$  and  $N_{\max}/N_0 = 100$  (subscript 0 refers to the reference case with half facet width  $R_0$  and subscript I indicates initial values). Here,  $E$  is Young's modulus,  $\Sigma_0 = (C^*/BI_n R_0)^{1/(n+1)}$  is the amplitude of the HRR-field measured at a distance  $R_0$  in front of the crack tip, and correspondingly  $\dot{E}_0 = B\Sigma_0^n$ ,  $N_0 = 1/(\pi R_0^2)$  and  $L_0 = (\mathcal{D}\Sigma_0/\dot{E}_0)^{1/3}$ . Figure 3a shows the cavitation state at  $t/t_{R0} = 1.86$  ( $t_{R0} = \dot{E}_0^{-1}$ ). The value of  $a/b$  is plotted perpendicular to each facet and with the ordinate along the facet. Wherever microcracking has occurred due to cavity coalescence at  $a/b = 0.7$ , this is highlighted in black. We see that the initially sharp crack has extended under an angle of approximately  $60^\circ$  by the linking-up of grain boundary microcracks and that the fracture process is rather ductile.

To analyze the effect of grain size, we consider two more cases with grain sizes  $R = 5R_0$  and  $R = 10R_0$ , respectively. The load parameter  $C^*$  and material parameters  $n$ ,  $a_I$ ,  $N_I$ ,  $E$ ,  $B$ ,  $\eta_B/w$ ,  $\mathcal{D}$  and  $N_{\max}$  are kept unchanged. However, the nucleation activity parameter  $F$  is tuned to the grain size in order to ensure that cavity size and density remain within realistic bounds. As will be pointed out in Sec. 4, this results in  $F = (R/R_0)F_0$ . Figure 3b shows the cavitation state in the material with the largest grain size at

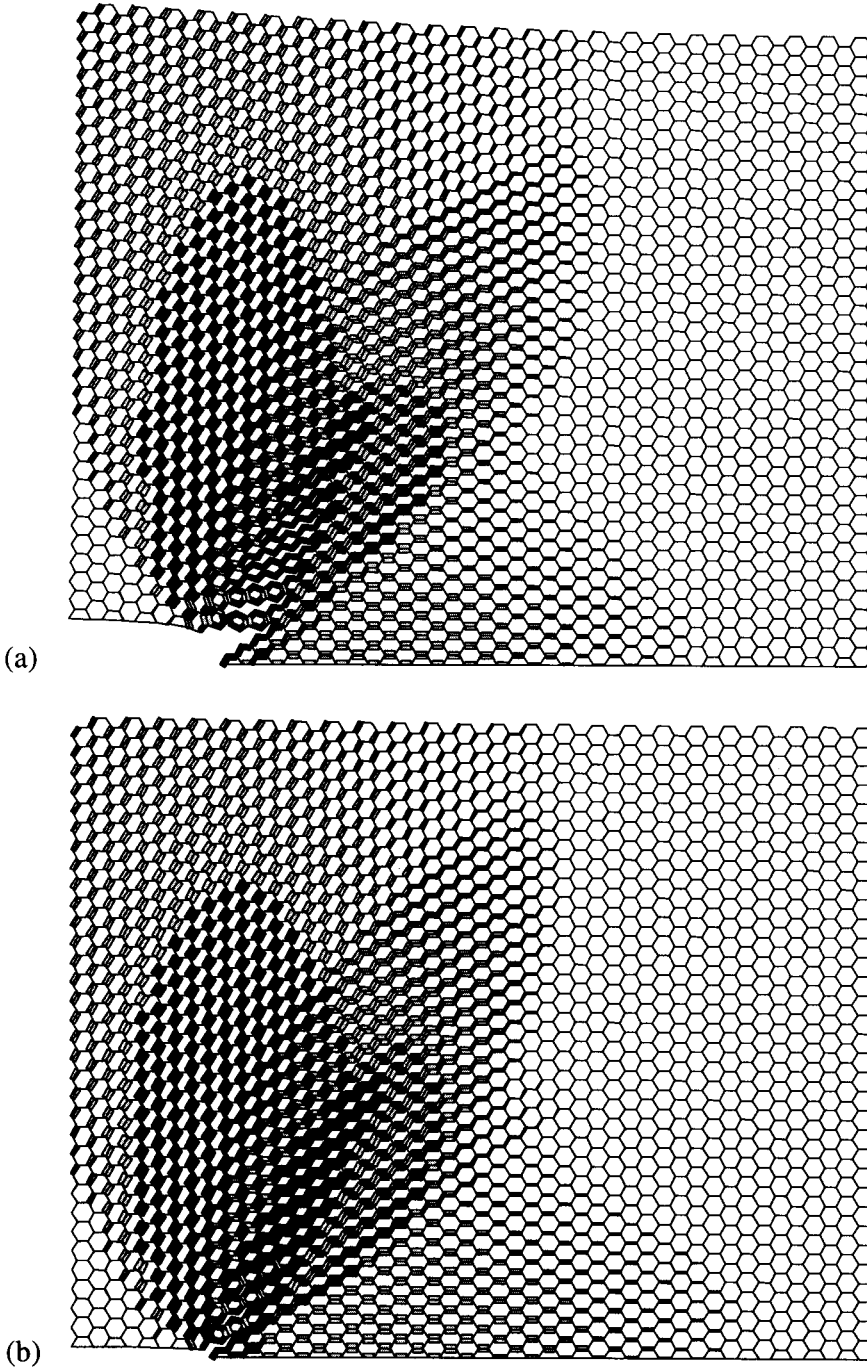


Figure 3: The damage state in the process window (see Fig. 2b). Values of  $a/b$  are plotted along and on either side of the grain boundary facets. Microcracked regions where  $a/b = 0.7$  are indicated by black. (a)  $R = R_0$ ,  $t/t_{R0} = 1.86$ ; (b)  $R = 10R_0$ ,  $t/t_{R0} = 2.95$ .

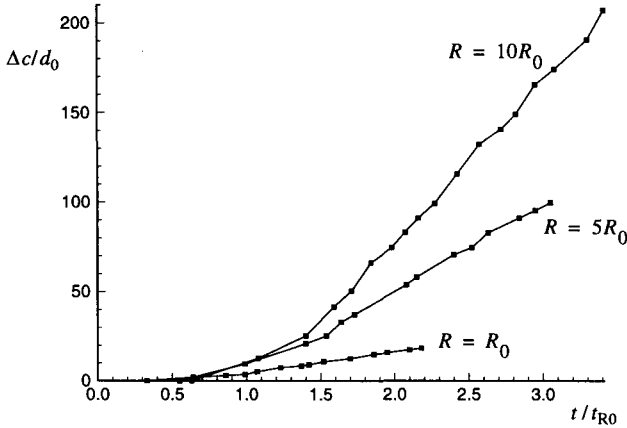


Figure 4: (a) Crack growth increment vs. time, normalized with respect to the reference case  $R = R_0$ .

$t/t_{R_0} = 2.95$ . Note that the damage zone is very similar in shape as that in Figure 3a and comprises approximately the same number of (larger) grains, while the fracture process is more brittle. Figure 4 shows the crack extension for all three grain sizes as a function of time, normalized with respect to quantities in the reference case. After an incubation period and accelerating growth, the crack growth rates approach constant values:  $\dot{c}_0/d_0 = 12.1$  ( $R = R_0$ ),  $\dot{c}_0/d_0 = 48.6$  ( $R = 5R_0$ ) and  $\dot{c}_0/d_0 = 89.1$  ( $R = 10R_0$ ), respectively, showing an increase in crack velocity with grain size. The crack tip opening rates,  $\dot{u}^{\text{ctod}}$  were found to be virtually identical for the three cases, indicating that the crack tip opening rate is controlled by the far field strain rate which is equal for all grain sizes. From Fig. 4 we can compute a 'brittleness factor' [7], defined as  $\dot{c}/\dot{u}^{\text{ctod}}$ , and find that this clearly increases with grain size.

#### 4 DISCUSSION

The preliminary results presented here are concerned with only a small subset of all possible size effects. With virtually all material constants being kept constant, the key size effect that is incorporated is the changing ratio between the grain size and the characteristic length in the gradients in the HRR stress field.

Careful investigation of the trends observed in Figs. 3–4 leads to the following interpretation. When one considers the same stress gradient acting over two microstructures with different grain size, the level of the facet normal stress at a given number of grain distances from the crack tip will be lower for the larger grain size. This can be expressed by

$$\Sigma = \left[ \frac{C^*}{BI_n R} \right]^{1/(n+1)} = \left[ \frac{R}{R_0} \right]^{-1/(n+1)} \Sigma_0. \quad (7)$$

As a result, the above-mentioned stress dependent non-dimensional parameters change as

$$\frac{\dot{E}}{\dot{\epsilon}_B} = \left[ \frac{R}{R_0} \right]^{\frac{-2n}{1-n}} \frac{\dot{E}_0}{\dot{\epsilon}_{B0}} = 2.6 \frac{\dot{E}_0}{\dot{\epsilon}_{B0}}, \quad \frac{a_1}{L} = \left[ \frac{R}{R_0} \right]^{\frac{1-n}{3(n+1)}} \frac{a_1}{L_0} = 0.6 \frac{a_1}{L_0}, \quad (8)$$

for  $R = 10R_0$  and  $n = 5$ . The increase in  $\dot{E}/\dot{\epsilon}_B$  indicates that the strain rate contribution of grain boundary sliding decreases with increasing grain size, which agrees with experimental observations [2, 10]. However, the effect on the overall strain rate is rather small [18]. The decrease in  $a_1/L$  indicates that the relative contribution of diffusion to cavity growth increases (see Sec. 2.1). Previous investigations (e.g. [14, 19]) have shown that this parameter is key in governing the brittleness of the damage process, suggesting that the brittleness increases with grain size. This is consistent with the findings above.

This interpretation can be further refined by considering the characteristic time scales involved. Creep crack growth is governed by three principal physical processes: cavity nucleation, diffusional cavity growth

Table 1: Classification of creep fracture in four limiting regimes, based on the characteristic time scales  $t_{\text{nuc}}$ ,  $t_{\text{dif}}$ ,  $t_{\text{coal}}$  and  $t_{\text{cr}}$  for nucleation, diffusion, coalescence and creep, respectively.

	small damage zone	large damage zone
brittle fracture	$t_{\text{nuc}} > t_{\text{dif}}$	$t_{\text{nuc}} < t_{\text{dif}}$
	$t_{\text{coal}} < t_{\text{cr}}$	$t_{\text{coal}} < t_{\text{cr}}$
ductile fracture	$t_{\text{nuc}} > t_{\text{dif}}$	$t_{\text{nuc}} < t_{\text{dif}}$
	$t_{\text{coal}} > t_{\text{cr}}$	$t_{\text{coal}} > t_{\text{cr}}$

and creep deformation, each with its own characteristic time scale:  $t_{\text{nuc}} = (l^2 \dot{N})^{-1}$ ,  $t_{\text{dif}} = l^3 / (\mathcal{D}\Sigma)$  and  $t_{\text{cr}} = \bar{E}^{-1}$ , respectively. Here,  $\dot{N} = F(\Sigma/\Sigma_0)^2 \dot{E}$  and  $l$  is a length scale associated with the grain boundary damage process (e.g.  $a_1, b_1$ ) and does not depend on grain size. Assuming that cavity growth is dominated by diffusion, the relative magnitude of  $t_{\text{nuc}}$  and  $t_{\text{dif}}$  determines whether cavities coalesce soon after nucleation or whether time elapses, allowing for a considerable damage zone to develop in front of the crack tip. Consequently, the characteristic time for cavity coalescence on a facet,  $t_{\text{coal}}$ , consists of time consumed by nucleation as well as growth:  $t_{\text{coal}} = t_{\text{nuc}} + t_{\text{dif}}$ . Then, the ratio of  $t_{\text{coal}}$  and  $t_{\text{cr}}$  determines whether creep deformation can accumulate during crack growth (resulting in ductile fracture) or whether fracture is brittle. Just as in [15], we can identify four limiting regimes, ranging from brittle fracture with a small damage zone to ductile fracture with a large damage zone. They are summarized in Table 1.

Further understanding of the numerical results can now be obtained by considering how a change in grain size will affect the relative contribution of the above three time scales. However, for the computations we assumed that the nucleation rate was coupled to the diffusional cavity growth rate, which was accomplished by adjusting the nucleation activity  $F$ . This corresponds to imposing  $t_{\text{nuc}} = t_{\text{dif}}$ , from which it follows that  $F = (R/R_0)F_0$ . As a consequence,  $t_{\text{nuc}}$  drops out as an independent time scale (cf. [15]), and also it explains the observation in Fig 3 that the shape of the damage zone is almost independent of grain size. Substitution of (7) yields

$$t_{\text{coal}} = 2 t_{\text{dif}} = 2 \left[ \frac{R}{R_0} \right]^{\frac{1}{n+1}} t_{\text{dif}}^0, \quad t_{\text{cr}} = \left[ \frac{R}{R_0} \right]^{\frac{n}{n+1}} t_{\text{cr}}^0, \quad (9)$$

resulting in

$$\frac{t_{\text{cr}}}{t_{\text{coal}}} = \left[ \frac{R}{R_0} \right]^{\frac{n-1}{n+1}} \frac{t_{\text{cr}}^0}{t_{\text{coal}}^0}. \quad (10)$$

This indicates that more brittle crack growth will occur (larger  $t_{\text{cr}}/t_{\text{coal}}$ ) if the grain size is increased. This too clearly corresponds with the findings in Fig. 3.

We can also rationalize the predicted grain size dependence of the crack growth velocity according to Fig. 4. To this end, we define the crack growth velocity as the reciprocal of the time required for cavity coalescence to take place along the entire facet, i.e.  $\dot{c} \propto R/t_{\text{coal}}$ . It follows that

$$\dot{c} = \left[ \frac{R}{R_0} \right]^{\frac{n}{n+1}} \dot{c}_0. \quad (11)$$

Using  $n = 5$  results in  $\dot{c} = 3.8 \dot{c}_0$  and  $\dot{c} = 6.8 \dot{c}_0$  for  $R = 5R_0$  and  $R = 10R_0$ , respectively. Despite the very approximate nature of these estimates, it agrees rather well with the computed values  $\dot{c} = 4.0 \dot{c}_0$  and  $\dot{c} = 7.3 \dot{c}_0$  from Fig. 4. This suggests that even though the actual stress distributions over the individual facets will not be uniform, it is the average value over the facet that primarily determines the time to formation of a facet microcrack. It should also be noted that this argument implies that the stress state near the tip of the propagating crack does not differ in nature from the HRR field; this is consistent with our finding that the cavitation damage process right near the crack tip is basically unconstrained [15].

The current microstructural model also features a possible grain size effect through the change in density of triple grain junctions. It has been suggested (e.g. [6, 10, 11]) that they act as barriers for crack advance

during the linking-up of microcracks. However, this effect cannot be readily separated in the numerical results from the other size effects.

Finally, we discuss the mere indirect effects of grain size through the nucleation rate and creep resistance, independent from the direct size effect as addressed in the simulations, by using  $R = R_0$ . An indirect effect of increasing the grain size can enter through an increase in the cavity nucleation rate (higher  $F$ , see e.g. [9]). Assuming nucleation and diffusional cavity growth to be uncoupled, this will decrease the characteristic time for nucleation,  $t_{\text{nuc}}$ , and thus increase the damage zone. Correspondingly, also the time for facet failure,  $t_{\text{coal}}$ , decreases, resulting in more brittle growth and an accelerated crack growth rate, which is in accordance with investigations in which a size effect is introduced by experimentally changing the grain size.

Another indirect effect is through the creep resistance, which either decreases or increases with grain size, depending on load level and temperature (e.g. [1]). This can be expressed by  $B = (R/R_0)^m B_0$ , where  $B_0$  is the creep parameter in the reference case. Clearly,  $m > 0$  corresponds to a grain boundary strengthening effect (like the Hall-Petch effect) while  $m < 0$  results in grain boundary softening. Substitution yields

$$t_{\text{nuc}} = \left[ \frac{R}{R_0} \right]^{-m} t_{\text{nuc}}^0, \quad t_{\text{dif}} = t_{\text{dif}}^0, \quad t_{\text{cr}} = \left[ \frac{R}{R_0} \right]^{-m} t_{\text{cr}}^0, \quad (12)$$

which results in (assuming  $t_{\text{dif}}^0 = t_{\text{nuc}}^0$ ):

$$\frac{t_{\text{nuc}}}{t_{\text{dif}}} = \left[ \frac{R}{R_0} \right]^{-m} \frac{t_{\text{nuc}}^0}{t_{\text{dif}}^0}, \quad \frac{t_{\text{cr}}}{t_{\text{coal}}} = \frac{2 \left[ \frac{R}{R_0} \right]^{-m} t_{\text{cr}}^0}{1 + \left[ \frac{R}{R_0} \right]^{-m} t_{\text{coal}}^0}. \quad (13)$$

Increasing the grain size causes a larger damage zone, more ductile growth and an increased crack growth rate for  $m > 0$ , while it causes an opposite effect for  $m < 0$ . Evidently, the effect of grain size on creep resistance alone cannot explain the experimental observations of a simultaneous increase of brittleness and of crack growth rate.

## References

- [1] Shahinian P., Lane J.R., *Trans. ASM* **45** (1953) 177–199.
- [2] Fang T-T, Murty K.L., *Mat. Sci. Eng.* **61** (1983) L7–L10.
- [3] Takahashi Y., Yamane T., *J. Mater. Sci.* **14** (1979) 2818–2824.
- [4] Han Y., Chaturvedi M.C., Cahoon J.R., *Scr. Metall.* **22** (1988) 255–260.
- [5] Kimura K., Ohi N., Shimazu K., Matsuo T., Tanaka R., Kikuchi M., *Scr. Metall.* **21** (1987) 19–22.
- [6] Fleck R.G., Cocks G.J., Taplin M.R., *Metall. Trans.* **1** (1970) 3415–3420.
- [7] Gooch D.J., Haigh J.R., King B.L., *Met. Sci.* **11** (1977) 545–550.
- [8] Hong S.H., Yu J., *Scr. Metall.* **23** (1989) 1057–1062.
- [9] Needham N.G., Gladham T., *Mater. Sci. Techn.* **2** (1986) 368–373.
- [10] Mannan S.L., Rodriguez P., *Met. Sci.* **17** (1983) 63–69.
- [11] Zhu S.M., Wang F.G., Zhu S.J., *Mater. Trans. JIM* **34** (1993) 450–454.
- [12] Hayhurst D.R., Morrison C.J., Brown P.R., *Creep in Structures 1980*, Ponter A.R.S., Hayhurst D.R., Eds. (Springer Verlag, Berlin, 1981), pp. 564–575.
- [13] Hall F.R., Hayhurst D.R., *Proc. Roy. Soc. Lond. A* **433** (1991) 405–421.
- [14] Onck P.R., Van der Giessen E. *Mech. Mater.* **26** (1997) 109–126.
- [15] Onck P.R., Van der Giessen E., *J. Mech. Phys. Solids*, (1997) submitted for publication.
- [16] Needleman A., Rice J.R., *Acta Metall.* **28** (1980) 1315–1332.
- [17] Tvergaard V., *J. Mech. Phys. Solids* **32** (1984) 373–393.
- [18] Van der Giessen E., Tvergaard V., *Int. J. Fract.* **48** (1991) 153–178.
- [19] Van der Giessen E., Tvergaard V., *Acta Metall. Mater.* **42** (1994) 959–973.